2013

The Effect of Ultrasound Stimulation on the Cytoskeletal Organization of Chondrocytes Seeded In 3D Matrices

Sandra Noriega
University of Nebraska-Lincoln

Gulnara Hasanova
University of Nebraska - Lincoln

Anuradha Subramanian
University of Nebraska-Lincoln, asubramanian2@unl.edu

Published in final edited form as:
Cells Tissues Organs. 2013 ; 197(1): 14–26. doi:10.1159/000339772.

The Effect of Ultrasound Stimulation on the Cytoskeletal Organization of Chondrocytes Seeded In 3D Matrices

Sandra Noriega, **Gulnara Hasanova**, and **Anuradha Subramanian**
Department of Chemical and Biological Engineering, University of Nebraska, Lincoln, Nebr., USA

Abstract

The impact of low intensity diffuse ultrasound (LIDUS) stimulation on the cytoskeletal organization of chondrocytes seeded in 3D scaffolds was evaluated. Chondrocytes seeded on 3D chitosan matrices were exposed to LIDUS at 5.0 MHz (~15kPa, 51-secs, 4-applications/day) in order to study the organization of actin, tubulin and vimentin. The results showed that actin presented a cytosolic punctuated distribution, tubulin presented a quasi parallel organization of microtubules whereas vimentin distribution was unaffected. Chondrocytes seeded on 3D scaffolds responded to US stimulation by the disruption of actin stress fibers and were sensitive to the presence of ROCK inhibitor (Y27632). The gene expression of ROCK-I, a key element in the formation of stress fibers and mDia1, was significantly up-regulated under the application of US. We conclude that the results of both the cytoskeletal analyses and gene expression support the argument that the presence of punctuated actin upon US stimulation was accompanied by the up-regulation of the RhoA/ROCK pathway.

Keywords

Actin cytoskeleton; Biomaterial; Cartilage articular; Cartilage research; Cell-cell and cell-matrix interactions; Cytoskeleton; Cytoskeleton interaction; Tissue engineering of cartilage and bone

Introduction

The mechanisms by which US stimulation induces mechanical stress may involve (a) receptor mediated transmembrane signaling mechanisms, (b) activation of the stretch-receptor ion channels (Mobasheri, Carter et al. 2002) and (c) a redistribution of the cytoskeletal elements coupled with a change in cellular morphology. We confine our research to the impact of US stimulation on the morphology and the cytoskeletal organization of chondrocytes maintained in 3D scaffolds. The cytoskeleton of a cell is an organized network of three main protein fibers: microfilaments (MF), microtubules (MT) and intermediate filaments (IF) each having specific cellular functions (Herrmann, Bär et al. 2007). MFs, which are mainly composed of β-actin subunits (Blain 2009) provide mechanical strength to the cell and act as a linker between transmembrane and cytoplasmic proteins. MTs, which are assemblies of α and β tubulin dimers are involved in the distribution of organelles and also drive ciliary movements, intracellular transport and cell division (Herrmann, Bär et al. 2007; Blain 2009). IFs, which are cell type–specific, connect the nuclear envelope to the cell membrane (Goldman, Grin et al. 2008). The latter have been reported to be involved in both signal transduction via integrins and in the direct transductions of cellular deformations to the nucleus (Langelier, Suetterlin et al. 2000).

Dr. Anuradha Subramanian Department of Chemical and Biological Engineering University of Nebraska Lincoln, NE 68516 (USA) Tel. +1 402 472 3463, asubramanian2@unl.edu.

Mesenchymal cells and chondrocytes contain vimentin as the IF (Benjamin, Archer et al. 1994).

Chondrocytes are mechano-responsive cells – a feature that is often exploited to grow tissue-engineered cartilage in *in-vitro* cultures under the influence of dynamic compression, rotation, hydrostatic pressure and ultrasound (Frondoza, Sohrabi et al. 1996; Carver and Heath 1999; Carver and Heath 1999a; Martin, Obradovic et al. 2000; Yamaoka, Asato et al. 2006). There has been keen interest in evaluating the effects of external stimuli on the biosynthetic activity of chondrocytes (Li, Danielson et al. 2003; Ng, Hung et al. 2007). The organization of the cytoskeleton under mechanical stress has been evaluated as well since the chondrocyte cytoskeleton is known to play a fundamental role in the control of the chondrocyte phenotype and in the interactions with the extracellular matrix (ECM). The cytoskeletal organization and composition of normal chondrocytes has been reported in detail (Langelier, Suetterlin et al. 2000), i.e. the distribution of actin is punctuated and dense at the peripheral cortex (Durrant, Archer et al. 1999; Langelier, Suetterlin et al. 2000; Trickey, Vail et al. 2004; Knight, Toyoda et al. 2006). MTs have been observed as a mesh spanning through the cytoplasm (Blain 2009) while IFs have been observed to form a mesh spanning through the cell nucleus to the cell membrane.

Chondrocytes subjected to mechanical compression (0.5MPa to 4 MPa) have produced changes in the cytoskeleton. Under the applied load the distribution of actin was not observed to change whereas the appearance of the vimentin network changed from being diffuse in appearance to an organized network (Durrant, Archer et al. 1999). Changes in actin and tubulin signal intensity upon the application of continuous high pressure (24 MPa) have been reported (Fioravanti, Benetti et al. 2005). Actin remodeling has been noted in cells subjected to compression or hydrostatic pressure under either static or cyclical conditions. With the exception of cells exposed to cyclical hydrostatic pressure, in all cases cytoskeletal organization has been observed to return to control levels one hour after loading (Knight, Toyoda et al. 2006). Further, stimulation of primary human skin fibroblasts via ultrasound (Langelier, Suetterlin et al. 2000) has been shown to impact cytoskeletal organization, where LIDUS induced the formation of actin stress fibers that was mediated by the activation of Rho-A (Zhou, Schmelz et al. 2004).

The effect of LIDUS stimulation on the proliferation, protein- and gene expression of chondrocytes seeded on 3D chitosan scaffolds has been reported elsewhere (Noriega, Mammedov et al. 2007; Hasanova, Noriega et al. 2010). Specifically, the gross morphology of chondrocytes was observed to be impacted by the frequency of the US signal employed (Hasanova, Noriega et al. 2007; Noriega, Mammedov et al. 2007). We hypothesize that US stimulation of chondrocytes triggers or facilitates an intracellular response which leads to a rearrangement of the cytoskeletal elements. We focus on tasks that will permit an evaluation of the impact of US stimulation on the cytoskeletal organization of chondrocytes maintained in 3-D scaffolds. The rationale underlying these experiments is that cytoskeletal elements play a significant role in mechanotransduction and that mechanical stimuli can affect the actin cytoskeleton (Campbell, Blain et al. 2007). Thus, a study of the in-situ distribution and physiological 3-D organization of chondrocyte cytoskeletal networks (MFs, MTs and vimentin IFs) upon US stimulation is essential for a better understanding of the role of the cytoskeleton under mechanical stimulation.

Materials and Methods

Scaffold preparation and cell seeding

Chitosan scaffolds (CS) were prepared by the freeze drying and lyophilization method as detailed elsewhere (Hasanova, Noriega et al. 2010), sterilized and pre-wetted with (DMEM/

F-12 with 10% FBS) prior to cell seeding experiments. Discarded tissue from the shoulder joints of young calves was obtained from a local abattoir and articular chondrocytes were extracted using the procedure detailed elsewhere (Hasanova, Noriega et al. 2010). Articular chondrocytes were grown in DMEM/F-12 in the presence of 10% fetal calf serum (GIBCO), 1% of non-essential amino acids (GIBCO), 2 mM L-glutamine and 1.0% of penicillin-streptomycin (Sigma Chemical Company, St. Louis, MO). All cells were grown at 37°C under a 5% CO_2-humidified atmosphere.

Pre-wetted scaffold discs (5mm × 2.5mm) were seeded with bovine chondrocytes from passage-3 at a seeding density of 3×10^4 cells/scaffold, with six scaffolds per well in a 6-well tissue culture plate. One plate with 36 scaffolds represented one test condition. Typically, 15 μl of a 2.0×10^6 cells/ml stock solution was pippeted on each scaffold and the plates were kept in the CO_2 incubator at 37°C and 95% RH for 3 hours. Next, 8-ml of fresh medium was added on top of the scaffolds and maintained for 20-hours in the incubator. The scaffolds were transferred to a new TCP-plate with 5-8 ml of fresh complete media per well and placed in the incubator. Control treatments did not include US stimulation and were handled similarly to US treated specimens. The medium was changed every alternate day. Unseeded disks were included as control.

MTT [3-(4,5-dimethylthiazol-2-yl)-2,5-diphenyl tetrazolium bromide] viability assay

Fifty μl of MTT solution (1mg/ml in phenol red free medium) was added to each well of a 96-well plate that contained a scaffold, followed by 4 hours of incubation in the CO_2 incubator. The solution was then removed and 100 μl of isopropanol per well was added. Upon incubation for 30 minutes, the absorbance at 570 nm was determined. Six to eight samples for each condition were analyzed.

Ultrasound stimulation

The LIDUS was used to excite the chondrocytes seeded in scaffolds. However, unlike previous studies, the total application time was quite long relative to the maximum travel time across the well (~ 35 μs), meaning that the cells were excited in an incoherent (diffuse) manner due to the numerous multiple reflections from the boundaries of the well that the US waves experienced. The maximum intensity was quantified using a needle hydrophone (Onda Corp., Sunnyvale, CA). Because the waves multiply-reflect from the boundaries, the maximum intensity was found by moving the hydrophone to many positions within the well and observing the complete time domain signal. The total stimulation time was chosen such that the number of cycles was approximately constant and of the same order as previous work (Parvizi, Wu et al. 1999). Non-stimulated cell-seeded scaffolds served as controls (denoted as control) and were handled identically to the LIDUS-stimulated scaffolds. The LIDUS excitation was sinusoidal at 5.0 MHz for 51 sec with maximum pressure amplitude of ~15kPa at any spatial position.

Chondrocytes seeded in 3D scaffolds were maintained in culture for 3 days and then stimulated with the US signal as indicated. The ultrasound was introduced into the wells using a nonfocused, immersion transducer (Panametrics, V300, Waltham, MA), 0.5 inch diameter, 5 MHz center frequency as described previously (Noriega, Mammedov et al. 2007). Ultrasound was applied 1X, 2X, 4X, and 8X per day. The time interval between applications was 7 hours, 3 hours and 1 hour for the 2X, 4X, and 8X application frequencies, respectively. The US transducer was directly applied over the medium above the scaffolds, the probe was positioned 10.5 mm above the well's bottom and the height of the medium in the well was kept at 12.0 mm. The probe was sterilized with ethanol before each application.

Typically, a total of 1.0-5.0 $\times 10^6$ chondrocyte cells was collected from 36 scaffolds (one test plate, one condition) after treatament. The cells were immediately frozen in liquid nitrogen and stored at −80°C until further use.

ROCK-I inhibitor

ROCK-I inhibitor (Y27632; TOCRIS-1254, MO) was added to each well of a 6-well TCP plate at a final concentration of 20 μM. The inhibitor was added every time the medium was changed on the plates subjected to the inhibition experiment.

mRNA gene expression analysis

RNA was extracted from liquid nitrogen-frozen cells using 1ml Trizol reagent (Invitrogen) and 250 μg/ml glycogen (Invitrogen) added as carrier. The integrity and purity of the isolated RNA isolated, typically, about 10 to 15 μg, were assessed by gel electrophoresis and A260/A280 absorbance ratios. Two μg of mRNA was used for making the cDNA templates. About 80-150 ng RNA/cDNA (cDNA corresponding to 80-150 ng total RNA) from each sample was used for PCR amplification of all genes. RNA samples (~2 μg) were pre-treated with 3 units of DNase I using the DNA-free kit (Invitrogen) for 20 min at room temperature, after which the enzyme was inactivated at 65°C in the presence of 2 mM EDTA. Then, the DNase- free RNA preparations were used for synthesis of the first-strand cDNA with 50 ng random hexamers primer and SuperScript II Reverse Transcriptase-based kit (Invitrogen, CA) at 42°C for 50 min. One (for GAPDH) or 3 μl microliter (for the remainder of the genes) of cDNA templates were expanded using the Tag DNA polymerase (Invitrogen) in each PCR reaction with 31 (for GAPDH) or 35-37 cycles (for the genes of interestgenes) of 94°C denaturation for 45 sec, a 55-60°C annealing period of 30 sec and a 72°C extension period of 1 min, and a final extension at 72°C for 10 min using the forward and reverse gene-specific primers, shown in Table 1. GAPDH, a housekeeping gene was used as a loading control. A series of PCR reactions was performed with the number of cycles as the variable to find the optimal cycle number for each individual gene. The optimal number of cycles for GAPDH was found to be 31 and between 35-37 cycles for the other genes assayed. The PCR products were analyzed on 1% agarose gels and stained with ethidium bromide. The band intensities on ethidium bromide-stained gels were quantified with the Alpha Innotech 8800 gel imaging system using Alpha EaseFC Software (Alpha Innotech, Santa Clara, CA).

Chondrocyte cell morphology on the samples

For SEM microscopy, the cells seeded in scaffolds were crosslinked with 2.5% glutaraldehyde (Sigma) in phosphate buffered saline (PBS) for 30 minutes, rinsed with deionized water and gradually dehydrated with a series of ethanol solutions. Hexamethyl disilazane (Fisher, PA) was used to remove 100% ethanol. Samples were sputter coated with Au-Pd prior to examination under SEM (Hitachi, S-3000N variable pressure, Japan). A voltage of 15 kV was used to visualize the samples.

Cytoskeleton immunostaining for confocal microscopy visualization

For fluorescent staining, the cells seeded in scaffolds were fixed in 4% paraformaldehyde (PFA) in PBS penetrated with 0.1% Triton X-100 (Sigma, MO) in PBS. Scaffolds were sectioned and incubated with anti-tubulin antibody (Sigma-Aldrich-T4026; dilution: 1:200) for 12 hours, rinsed and labeled first with Alexa-488 (Invitrogen-A11001; dilution 1:200) for 12 hours, copiously rinsed and labeled with actin specific phalloidin-633 (Invitrogen-A22284; dilution 1:200) and Cy3 labeled anti-vimentin (Sigma-Aldrich-C9080; dilution 1:100) antibodies for 12 more hours?. Prior to confocal microscopy, the nuclei were counterstained with DAPI (Invitrogen-D1306; 0.05mg/ml) (excitation/emission maxima:

358/461 nm) before mounting on coverslips. A confocal laser scanning microscope Olympus Inverted (Olympus IX 81) was used to obtain the images. Laser lines 405 (DAPI), 488 (Alexa-488), 543 (Cy3) and 633 (Alexa-633) were used sequentially to obtain the corresponding scans. Acquisition functions including 3D construction, "z" series sectioning, time series observations, sequential laser scan and image analysis functions were used as appropriate. ImageJ™ software was used to build the montage of images out of the z slices obtained for each condition.

Quantification analysis

Band intensities were quantified by densitometry using ImageQuant software (v5.2, Molecular Dynamics, Sunnyvale, CA). The values reported were normalized to unstimulated controls. For the analysis of the US stimulation effects on mRNA levels, the data represented the mean and standard deviation values of 3 independent estimations.

Statistical analyses

Unless otherwise indicated, all experiments were run at least 3 times. One-way analysis of variance (ANOVA) followed by Tukey's post hoc test was performed for statistical analysis of data. $P < 0.05$ (compared to control) was considered significant.

Results

While US has been shown to impact cartilage function at the cellular level (Parvizi, Wu et al. 1999; Nishikori, Ochi et al. 2002; Zhang, Huckle et al. 2002; Zhang, Huckle et al. 2003), more research is necessary to understand the effect of US stimulation on chondrocytes seeded and maintained in 3-D scaffolds, which are better representatives of chondrocytes' *in-vitro* culture. To stimulate chondrocytes seeded in 3-D scaffolds, this study used a continuous ultrasound wave for a predetermined time interval (5.0HZ, 51secs, ~15kPa) rather than pulsed-ultrasound (1.5MHz, 6-40 mins) used in previous studies.

Gene expression of RhoA, ROCK-I and mDia1

ROCK-I is a key element in the formation of stress fibers; hence the gene expression of both ROCK-I and mDia1 were analyzed to ascertain the role, if any, of ROCK-I and mDia1 on cellular activity as shown in Figure 1. The impact of US stimulation on the mRNA expression was examined by RT-PCR as a function of the frequency of US application and normalized with respect to GAPDH. The results are presented in Figure 1A. Compared to the control, a higher level of ROCK-I, Rho-A and mDia1 mRNA expression was observed when the cells were stimulated with US 4X, and 8X per day, respectively. As reported elsewhere, the cells stimulated 4X per day showed a significant increase in viability compared to control (*$p<0.01$) (Hasanova, Noriega et al. 2010), while the cells stimulated 8X per day were not statistically different from controls. Therefore, the cells were stimulated 4X per day with the specified US regimen in all further experiments.

The observation that the gene expression of Rho-A and ROCK-I were impacted by ultrasound led to two hypotheses: that an effect on actin would be visible upon ultrasound stimulation, and that ROCK-I would be one of the main effectors of US on the cytoskeleton. To test these hypotheses, the cells were seeded in scaffolds and US stimulation was applied both in the presence and absence of Y27632, a ROCK-I inhibitor which has been shown to disrupt actin filaments (Riveline, Zamir et al. 2001).

Determination of cellular viability

Figure 2 shows the cell viability both in the presence and absence of the ROCK-I inhibitor, where the addition of Y27632 did not negatively impact the viability. The high cellular

viability (* $p < 0.01$) obtained in US stimulated cells was in agreement with previous results (Noriega, Mammedov et al. 2007).

Scanning electron microscopy

Figure 3 shows the gross morphology of the cells. Panel-A shows that the control cells without Y27632 presented a rounded morphology with some development of lamellipodia. Panel-B shows that the control cells with Y27632 presented a morphology of long thin extensions which is characteristic of cells with inhibited ROCK-I expression (Darenfed, Dayanandan et al. 2007). Panel-C shows that the US stimulated cells without Y27632 presented morphology of spindle-like shapes and the presence of long processes. Panel-D shows that the US cells with Y27632 presented morphology of much longer thin extensions than the non-stimulated control cells with Y27632.

Cytoskeletal analysis

Confocal microscopy was used to assess the distribution and organization of the chondrocyte cytoskeleton. Determinations were made before and after US stimulation, and in the presence and absence of the Y27632 inhibitor. Figure 4 shows the confocal images obtained. Panel-A (control cells) shows the presence of the long actin fibers which ran the length of the cells and an actin mesh surrounding the cells. Panel-B shows that the control cells with Y27632 had punctuated actin, and in some cases only membrane accumulated actin and no fibers, were detected, which confirms the disruption of actin fibers by the inhibitor. Panel C shows that in US stimulated cells without Y27632 the actin structure appeared to be non-organized and exhibited punctuated membrane and cytosolic located F-actin. There were only a few long actin filaments along with mesh-like actin structures; however, no stress fibers were observed. Panel D shows that the distribution of actin in US stimulated cells in the presence of Y27632 possessed some stress fibers as well as the presence of some long processes and microspikes.

Panel E shows the distribution of tubulin in the control cells without Y27632, which formed a mesh-like structure with fibers spanning the whole length of the cells. Panel F shows that the tubulin organization in the control cells with Y27632 was not impacted, although some fiber bundling was evident. Panel G shows that the tubulin network in the US stimulated cells was intact, and that there was no disruption in the organization of the tubulin bundles. However, with US stimulation, the tubulin seemed to acquire some organization in the form of parallel fibers. Panel H shows that the distribution of tubulin in US stimulated cells with Y27632 exhibited features similar to panel E.

Panel I shows the distribution of vimentin in control cells without Y27632. Vimentin was observed to form a mesh-like structure around and in very close contact with the nucleus spanning the whole cytoplasm, which was similar to the distribution reported elsewhere in native chondrocytes (Durrant, Archer et al. 1999). Panel J shows that the overall distribution of vimentin in control cells with Y27632 was not impacted, although some fiber bundling was evident. Panel K shows that the network distribution of vimentin in US stimulated cells without Y27632 was intact and that no fiber disruption was evident. Panel K shows that the network distribution of vimentin in US stimulated cells with Y27632 showed no significant change. Finally, no significant difference was noted in the images of DAPI stained nuclei between the various study groups (images not shown).

Figure 5A/B/C/D shows the montage made out of the “z” slices from the confocal images. Figure 5A shows the z slice of control cells without Y27632. Actin distribution was noted to be cortical, with some faint organization in a mesh-like structure. Figure 5B shows the montage made out of the control cells with Y27632; the cell shape was completely changed,,

i.e. flattened, and there were more cell processes. Moreover, the actin filaments were completely disrupted and the actin distribution was even throughout the cytoskeleton. Figure 5C shows the montage made out of the z slices from the confocal images taken from US stimulated cells without Y27632; the cell shape was also elongated. The white arrow on the image shows some cytoplasmic punctuated actin (Haudenschild, D'Lima et al. 2008). Figure 5D shows that the montage made out of the z slices from the confocal images of cells taken from US stimulated cells with Y27632, was similar to that for the control cells with Y27632, except that the cell shape was stellar in shape and not spindle-like. Further, actin stress fibers and cytoplasmic actin were not detected.

In order to evaluate the time-dependent effect of ultrasound, the cytoskeleton organization and chondrocytes seeded on scaffolds were stimulated with US for 1-, 3- and 7- days. Figure 6 Panels A, B, and C show the images of tubulin cytoskeleton for the non-US stimulated control cells after 1-, 3- and 7- days, respectively. MTs were noted to span the length of the cell, from the microtubule organizing center (MTOC) to the ends of the cells, as can be observed in the inset. No evident organization of MTs was observed. Figure 6 Panels D, E, and F show the images of tubulin cytoskeleton for the US-stimulated cells after 1-, 3- and 7- days, respectively. MTs showed a weak organization and seemed to start acquiring a parallel distribution. No obvious change in the organization and distribution of vimentin was observed between the control and US-stimulated cells (images not shown).

Actin cytoskeleton was also analyzed and observations similar to those in Figure 5 were noted, i.e. the distribution of actin in the control cells was cortical, with some mesh-like structures, whereas US-stimulated cells had stress fibers that were mostly disrupted. As mentioned, this study also evaluated the time-dependent effect of ultrasound on the cytoskeleton organization and chondrocytes seeded on scaffolds. Figure 6 Panels A, B, and C shows the images of tubulin cytoskeleton for the non-US stimulated control cells after 1-, 3- and 7- days, respectively. MTs were noted to span the length of the cell, from the microtubule organizing center (MTOC) to the ends of the cells, as can be observed in the inset. No evident organization of MTs was observed. Figure 6 Panels D, E, and F shows the images of tubulin cytoskeleton for the US-stimulated cells after 1-, 3- and 7- days, respectively. MTs showed a weak organization and seemed to start acquiring a parallel distribution. No obvious change in the organization and distribution of vimentin was observed between the control and US-stimulated cells (images not shown).

Actin cytoskeleton analysis showed observations similar to those in Figure 5, i.e. the distribution of actin in the control cells was cortical, with some mesh-like structures, whereas the US-stimulated cells had stress fibers that were mostly disrupted.

Discussion

It has been postulated that the Rho family of small GTPases and downstream targets such as Rho activated kinase-1 (ROCK-I) and mDia1 regulate cytoskeletal organization (Watanabe, Kato et al. 1999), in particular, the formation of stress fibers and focal adhesion complexes (Riveline, Zamir et al. 2001). The organization and redistribution of cytoskeletal elements, notably actin, was noted to be impacted by US stimulation. The distribution of actin in chondrocytes seeded on 3-D chitosan-based scaffolds without any US stimulation, which served as controls, resembled the distribution of actin in 3-D agarose gel-based matrices, where the actin was observed to be cortical and formed a mesh-like structure around the cytoplasm (Idowu, Knight et al. 2000; Knight, Toyoda et al. 2006). As anticipated, the addition of the actin inhibitor, Y27632, disrupted the actin organization and the stress fibers in control cells, and resulted in an elongated cellular morphology. Surprisingly, cells subjected to US stimulation also exhibited an altered actin distribution; namely, no fiber-like

structure and an elongated shape when compared to the control cells. The actin structure in the cells that were subjected to US stimulation in the presence of Y27632 inhibitor was noted to be similar to the non-stimulated cells that were cultured in the presence of the actin inhibitor (figure-5/panel-D). The actin structure was similar in both the US-stimulated and non-stimulated cells with Y27632 (Figure 5 Panel D).

Previous work has reported on the reorganization of actin when chondrocytes embedded in agarose were subjected to dynamic compression (0.5 Hz at a 5-15% strain simulating a sinusoidal wave) (Haudenschild, D'Lima et al. 2008). Specifically, cytoskeletal rearrangements of actin, which mainly included a significant increase in F-punctuated actin, were noted and interestingly, Rho kinase appeared to mediate the observed changes in actin organization (Haudenschild, D'Lima et al. 2008). For example, upon dynamic compression for 10-min, a 3-fold increase in the levels of Rho-GTP and punctuated, cytosolic F-actin were noted when compared to the control cells. Interestingly, no punctuated actin was detected when the cells were subjected to dynamic compression in the presence of ROCK-I inhibitor, Y27632, (Haudenschild, D'Lima et al. 2008). This observation lends credence to the thought that ROCK (Rho associated kinase) is involved in the reorganization of actin. As shown in Figure 5 Panel-C, our study observed cytosolic punctuated actin in US-stimulated cells compared to the control cells where cortical actin was noted. We suggest that this supports the hypotheses that chondrocytes seeded on 3D scaffolds respond to US stimulation by the disruption of actin stress fibers and perhaps in a ROCK-I dependent manner. Interestingly, as noted in Figure 1, both the ROCK-I and the Rho-A genes were significantly up-regulated under the application of US. Both the cytoskeletal analyses and the gene expression support the theory that the presence of punctuated actin upon US stimulation is accompanied by the up-regulation of the RhoA/ROCK-I pathway.

In contrast to our observations, the development of actin stress fibers (Zhou, Schmelz et al. 2004) along with an up-regulation of Rho-A/ROCK-I pathway has been reportedwhen monolayer cultures of human fibroblasts are subjected to pulsed ultrasound (1.5 MHz, 1.0 kHz repeat, 10 mins/application). We believe that the differences can be assigned to the varied geometry of the support matrix, namely, 2D vs 3D support. In an independent experiment we observed distinct actin stress fibers and focal adhesions when chondrocytes were cultured on glass slides for 3 days (data not shown). In contrast, we observed a mixed population of cells with varying actin distributions, with the most representative distribution being cortical actin, when chondrocytes were cultured in 3D chitosan-based scaffolds.

A significant result of this study is the up-regulation in the gene expression of mDia1. One unexpected observation is the quasi parallel organization of MTs in the presence of ultrasound field. The self-organization of MTs *in vitro* has been shown to be gravity dependent (Papaseit, Pochon et al. 2000; Tabony, Glade et al. 2002), while numerical simulations of microtubule orientations suggest that the self-organization derives from the formation of the anisotropic chemical trails produced by the growth and shrinking of MTs. The process of tubulin polymerization and depolymerization creates concentration gradients that can activate and inhibit the formation of neighboring MT and induce MT organization (Tabony, Glade et al. 2002). Self-organization has been probed dependent on confinement limits (Pinot, Chesnel et al. 2009), forces (Janson, de Dood et al. 2003) and also on the presence of cations (Needleman, Ojeda-Lopez et al. 2004). The prediction that self-organization can be dependent on weak external fields (Tabony, Glade et al. 2002) is in line with our observations, i.e. MT organization was affected by ultrasound and MT alignment was noted in cells that underwent ultrasound stimulation.

In conclusion, LIDUS (~15 kPa) was shown to modulate the cytoskeleton organization of bovine chondrocytes maintained in 3D matrices. RT-PCR analysis revealed that US

stimulation treatment affected the expression of Rho-A, ROCK-I and mDia1. Our results confirm the important role of cytoskeleton in mediating the cellular responses to external stimuli.

Acknowledgments

We are especially thankful to Ms. Terry Fangman and the microscopy facility at the University of Nebraska, Lincoln, for their help with the confocal microscopy, image acquisition and processing. This research work was partially supported by UNL-Tobacco Settlement Funds, NIH grant:R21EB006046 and in part, by the American Recovery and Reinvestment Act of 2009 research grant 1R21RR024437-01A1 from the Department of Health and Human Service.

Abbreviations used in this paper

LIDUS	low intensity diffuse ultrasound
2D	two dimensional
3D	three dimensional
US	ultrasound
MF	microfilaments
MT	microtubules
IF	intermediate filaments
ECM	extracellular matrix
RH	relative humidity
TCP	tissue culture polystyrene
mRNA	messenger RNA
cDNA	complimentary DNA
SEM	scanning electron microscopy
GAPDH	Glyceraldehyde 3-phosphate dehydrogenase
PFA	paraformaldehyde
MTOC	microtubule organizing center
RT-PCR	reverse transcriptase polymerase chain reaction

References

Benjamin M, Archer CW, et al. Cytoskeleton of cartilage cells. Microscopy Research and Tecnique. 1994; 28:372–377.

Blain E. Involvement of the cytoskeletal elements in articular cartilage homeostasis and pathology. International Journal of Experimental Pathology. 2009; 90:1–15. [PubMed: 19200246]

Blain E. Involvement of the cytoskeletal elements in articular cartilage homeostasis and pathology. International Journal of Experimental Pathology. 2009; 90:1–15. [PubMed: 19200246]

Brown PD, Benya PD. Alterations in Chondrocyte cytoskeletal architecture during phenotypic modulation by Retinoic acid and Dihydrocytochalasin B-induced Reexpression. The Journal of Cell Biology. 1988; 106:171–179. [PubMed: 3276712]

Campbell JJ, Blain EJ, et al. Loading alters actin dynamics and up-regulates cofilin gene expression in chondrocytes. Biochem. and Biophys. Res. Comm. 2007; 361:329–334. [PubMed: 17662250]

Carver SE, Heath CA. Increasing Extracellular Matrix Production in Regenerating Cartilage with Intermitent Physiological Pressure. Biotechnol. Bioeng. 1999; 62:166–174. [PubMed: 10099526]

Carver SE, Heath CA. Semi-continuous perfusion system for delivering intemittent physiological pressure to regenarating cartilage. Tissue Engineering. 1999a; 5(1):1–11. [PubMed: 10207185]

Darenfed H, Dayanandan B, et al. Molecular Characterization of the Effects of Y27632. Cell Motility and the Cytoskeleton. 2007; 64:97–109. [PubMed: 17009325]

Durrant LA, Archer CW, et al. Organisation of the chondrocyte cytoskeleton and its response to changing mechanical conditions in organ culture. J. Anat. 1999; 194:343–353. [PubMed: 10386772]

Fioravanti A, Benetti D, et al. Effect of continuous high hydrostatic pressure on the morphology and cytoskeleton of normal and osteoarthritic human chondrocytes cultivated in alginate gels. Clinical and Experimental Rheumatology. 2005; 23:847–853. [PubMed: 16396703]

Frondoza C, Sohrabi A, et al. Human chondrocytes proliferate and produce matrix components in microcarrier suspension culture. Biomaterials. 1996; 17(9):879–888. [PubMed: 8718933]

Goldman RD, Grin B, et al. Intermediate filaments: versatile building blocks of cell structure. Current Opinion in Cell Biology. 2008; 20:28–34. [PubMed: 18178072]

Hasanova G, Noriega SE, et al. Effect of ultrasound stimulation on the biosynthetic activity of chondrocytes in cell-seeded matrices. European Cells and Materials. 2007; 14(Supp 3):108.

Hasanova GI, Noriega SE, et al. The effect of the indirect mechanical stimulation via ultrasound on the gene and protein expression of chondrocytes seeded in chitosan scaffolds. Journal of Tissue Engineering and Regenerative Medicine. 2010 (Accepted and In Press, 2010).

Haudenschild DR, D'Lima DD, et al. Dynamic compression of chondrocytes induces a Rho kinase-dependent reorganization of the actin cytoskeleton. Biorheology. 2008; 45:219–228. [PubMed: 18836226]

Herrmann H, Bär H, et al. Intermediate filaments: from cell architecture to nanomechanics. Nature Reviews: Molecular Cell Biology. 2007; 8:562–573.

Hu S, Chen J, et al. Cell spreading controls balance of prestresses by Microtubules and Extracellular Matrix. Frontiers in Bioscience. 2004; 9:2177–2182. [PubMed: 15353279]

Idowu B, Knight MM, et al. Confocal analysis of cytoskeletal organisation within isolated chondrocyte sub-populations cultured in agarose. The Histochemical Journal. 2000; 32:165–174. [PubMed: 10841311]

Ingber DE. Tensegrity I. Cell structure and hierarchical systems biology. Journal of cell Science. 2003; 116:1157–1173. [PubMed: 12615960]

Ishizaki T, Morishima Y, et al. Coordination of microtubules and the actin cytoskeleton by the Rho effector mDia1. Nature Cell Biology. 2001; 3:8–14.

Janson M, de Dood ME, et al. Dynamic instability of microtubules is regulated by force. The Journal of Cell Biology. 2003; 161(6):1029–1034. [PubMed: 12821641]

Knight MM, Toyoda T, et al. Mechanical compression and hydrostatic pressure induce reversible changes in actin cytoskeletal organisation in chondrocytes in agarose. Journal of Biomechanics. 2006; 39:1547–1551. [PubMed: 15985265]

Langelier E, Suetterlin R, et al. The chondrocyte cytoskeleton in Mature articular cartilage: Structure and Distribution of Actin, Tubulin and Vimentin Filaments. The Journal of Histochemistry and Cytochemistry. 2000; 48(10):1307–1320. [PubMed: 10990485]

Langelier E, Suetterlin R, et al. The chondrocyte cytoskeleton in mature articular cartilage: structure and distribution of actin, tubulin, and vimentin filaments. J Histochem Cytochem. 2000; 48(10): 1307–1320. [PubMed: 10990485]

Li WJ, Danielson KG, et al. Biological Response of chondrocyte culture in Three-Dimensional Nanofibrous Poly(e-caprolactone) scaffolds. Journal of Biomedical Materials Research. 2003; 67A:1105–1114. [PubMed: 14624495]

Mammoto A, Huang S, et al. Role of RhoA, mDia and ROCK in cell shape - dependent control of the Skp2-p27kip1 pathway and the G1/S transition. The Journal of Biological Chemistry. 2004; 279(25):26323–26330. [PubMed: 15096506]

Martin I, Obradovic B, et al. Modulation of the Mechanical Properties of tissue engineered cartilage. Biorheology. 2000; 37:141–147. [PubMed: 10912186]

Mobasheri A, Carter SD, et al. Integrins and stretch activated ion channels; putative compontnes of functional cell surface mechanoreceptors in articular chondrocytes. Cell Biology International. 2002; 26(1):1–18. [PubMed: 11779216]

Needleman DJ, Ojeda-Lopez MA, et al. Higher-order assembly of microtubules by counterions: From hexagonal bundles to living necklaces. PNAS. 2004; 101(46):16099–16103. [PubMed: 15534220]

Ng L, Hung H-H, et al. Nanomechanical properties of individual chondrocytes and their developing growth factor-stimulated pericellular matrix. Journal of Biomechanics. 2007; 40:1011–1023. [PubMed: 16793050]

Nishikori T, Ochi M, et al. Effects of low-intensity pulsed ultrasound on proliferation, and chondroitin sulfate synthesis of cultured chondrocytes embedded in Atelocollagen gel. Journal of Biomedical Materials Research. 2002; 59(2):201–206. [PubMed: 11745554]

Noriega SE, Mammedov T, et al. Intermittent Applications of Continuous Ultrasound on the viability, proliferation, morphology and Matrix production of chondrocytes in 3D matrices. Tissue Engineering. 2007; 13(3):611–618. [PubMed: 17518607]

Papaseit C, Pochon N, et al. Microtubule self-organization is gravity-dependent. PNAS. 2000; 97(15): 8364–8368. [PubMed: 10880562]

Parvizi J, Wu C, et al. Low-Intensity Ultrasound Stimulates proteoglycan synthesis in rat chondrocytes by increasing Aggrecan Gene Expression. Journal of Orthop. Res. 1999; 17:488–494. [PubMed: 10459753]

Parvizi J, Wu C, et al. Low intensity ultrasound stimulates proteoglycan synthesis in rat chondrocytes by increasing aggrecan gene expression. J. Orthop. Res. 1999; 17:487–494.

Pinot M, Chesnel F, et al. Effects of confinment on the self-organization of microtubules and motors. Current Biology. 2009

Putnam AJ, Schultz K, et al. Control of Microtubule Assembly by Extracellular Matrix and Externally Applied Strain. American Journal of Physiology. 2001; 280:C556–C564. [PubMed: 11171575]

Riveline D, Zamir E, et al. Focal contacts as Mechanosensors: Externally applied local mechanicla force induces growht of focal contacts by and mDia1-dependent and ROCK-independent mechanism. The Journal of Cell Biology. 2001; 153(6):1175–1185. [PubMed: 11402062]

Tabony J, Glade N, et al. Biological self-organization by way of microtubule reaction-diffusion processes. Langmuir. 2002; 18:7196–7207.

Trickey WR, Vail TP, et al. The role of the cytoskeleton in the Viscoelastic Properties of Human Articular Chondrocytes. Journal of Orthopaedic Research. 2004; 22:131–139. [PubMed: 14656671]

Wang N, Butler JP, et al. Mechanotransduction across the cell surface and through the cytoskeleton. Science. 1993; 260:1124–1127. [PubMed: 7684161]

Watanabe N, Kato T, et al. Cooperation between mDia1 and ROCK in Rho-induced actin reorganization. Nature Cell Biology. 1999; 1:136–143.

Yamaoka H, Asato H, et al. Cartilage Tissue Engineering using Human Articular Chondrocytes embedded in different hydrogel Materials. Journal of Biomedical Materials Research. 2006; 78A: 1–11. [PubMed: 16596585]

Zhang Z, Huckle J, et al. The influence of pulsed low-intensity ultrasound on matrix production of chondrocytes at different stages of differentiation: An explant study. Ultrasound Med. Biol. 2002; 28:1547–1553. [PubMed: 12498950]

Zhang Z, Huckle J, et al. The effects of pulsed low-intensity ultrasound on chondrocyte viability, proliferation, gene expression and matrix production. Ultrasound Med. Biol. 2003; 29(11):1645–1651. [PubMed: 14654159]

Zhou S, Schmelz A, et al. Molecular mechanisms of low intensity pulsed ultrasound in human skin fibroblasts. The Journal of Biological Chemistry. 2004; 279(52):54563–54469.

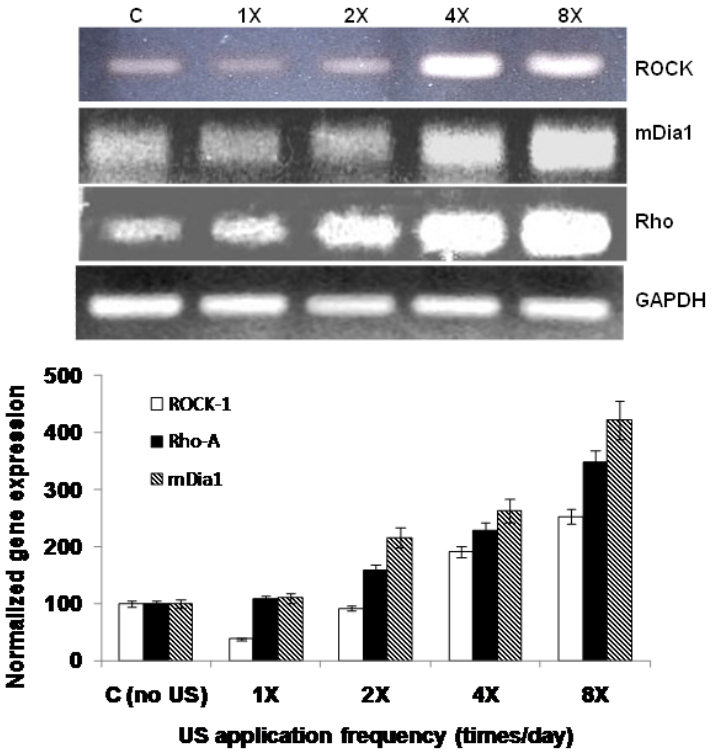

Figure 1. Analysis of the molecular responses of chondrocytes cultured in chitosan scaffolds to US stimulation

A 5.0 MHz US signal (~15kPa) was applied 1X, 2-X, 4X and 8X per day, 51 sec per application for one day. The mRNA levels of indicated genes (RhoA, ROCK-1 and mDia1) were measured by RT-PCR using the specific primers listed in Table 1. GAPDH **gene** was used **as a loading control.** Cells from seeded scaffolds that were not subjected to US stimulation served as controls. Data were normalized to the controls and are reported as a mean of three independent estimations with error bars, where an error bar represents one standard deviation.

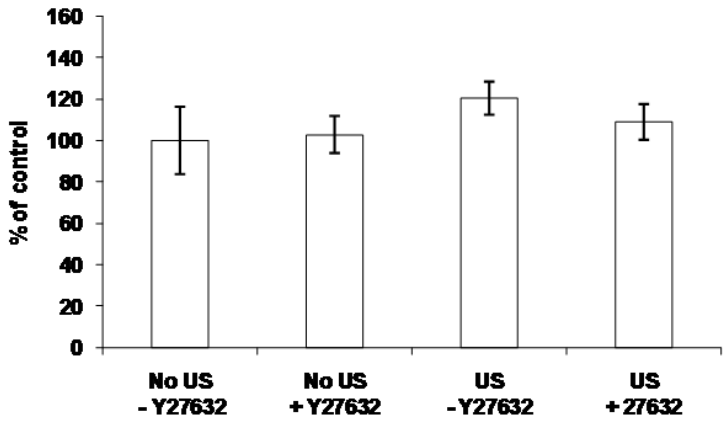

Figure 2. Effect of ROCK-1 (Y27632) inhibitor on cell viability

US signal was applied to cell-seeded chitosan scaffolds as follows: 4X per day, 51 sec per applications. Upon completion of the experiment, the cells seeded on scaffolds were subjected to US stimulation and the cellular viability was measured by MTT assay.

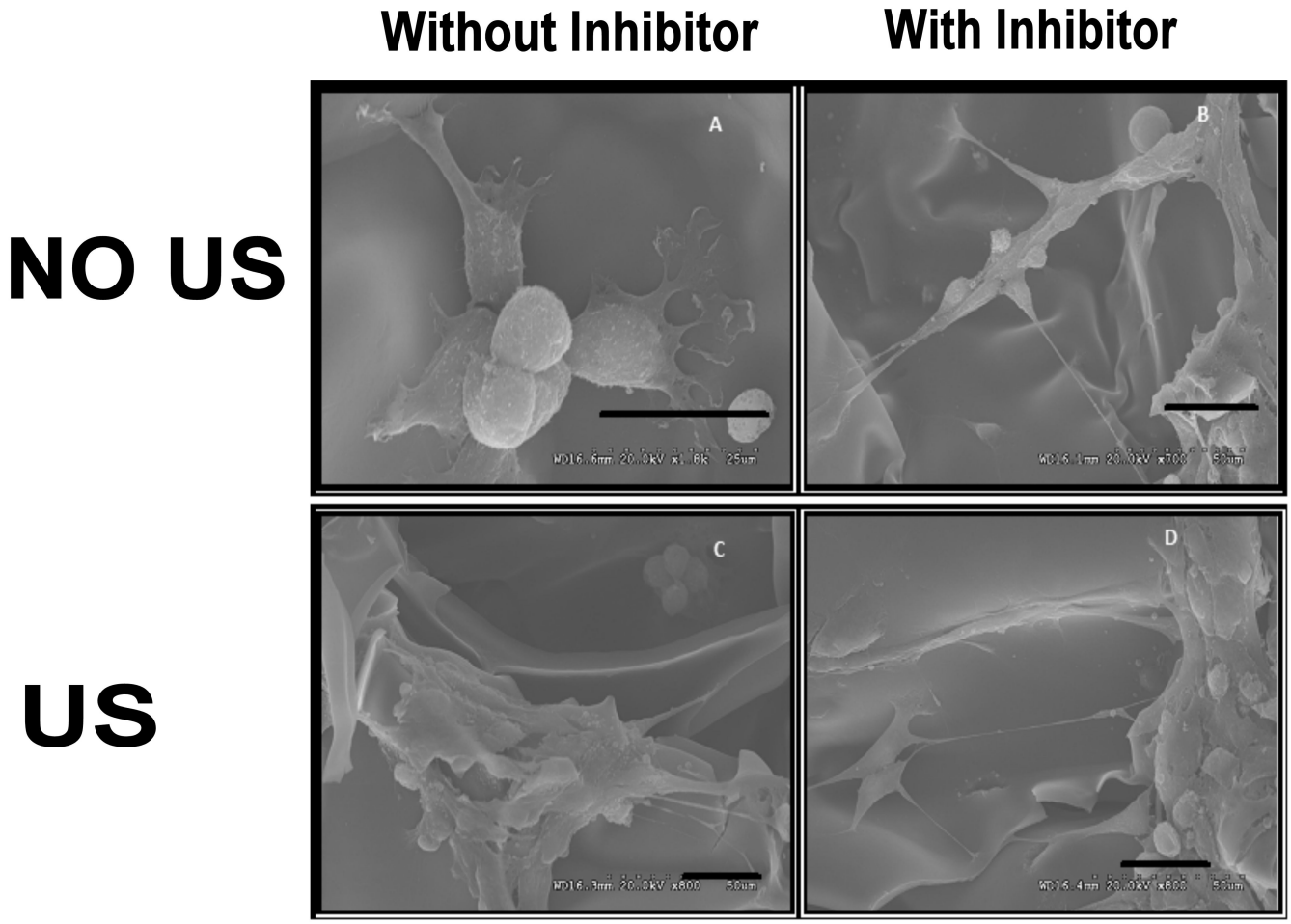

Figure 3. Effect of ROCK-1 (Y27632) inhibitor on cell gross morphology

US signal was applied to cell-seeded chitosan scaffolds as follows: 4X per day, 51 sec per application and maintained in culture in the presence and absence of the ROCK-1 inhibitor, Y26732. Upon completion of the experiment, the cell-seeded scaffolds were fixed and visualized by scanning electron microscopy. A) control cells in the absence of Y26732; B) control cells in the presence of Y26732; C) US-stimulated cells; d) US-stimulated cells in the presence of Y26732. Scale bar: 25 μm. Magnifications: (A) 1200X; (B) 700X; (C) 800X and (D) 800X.

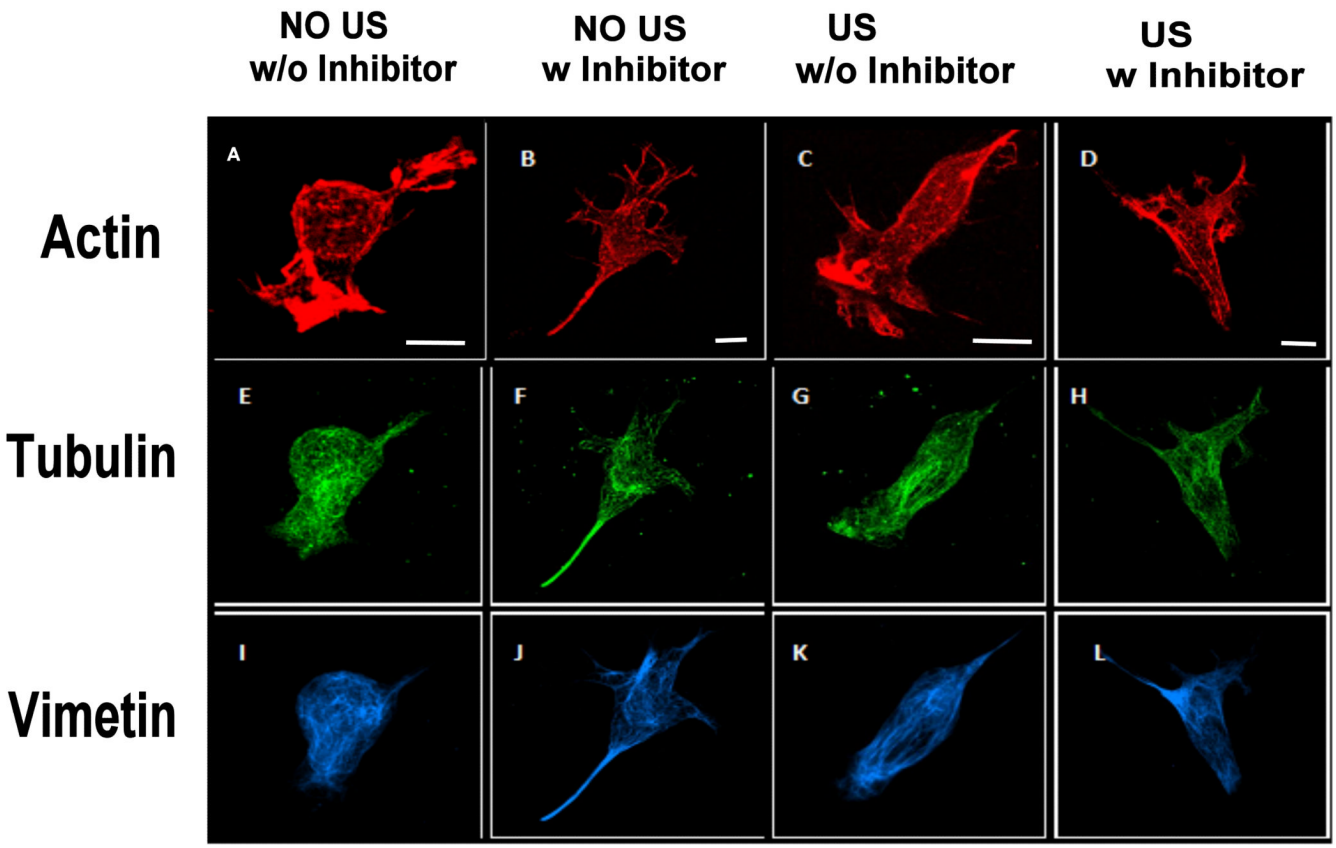

Figure 4. Visualization of chondrocyte cytoskeleton

US signal was applied to cell-seeded chitosan scaffolds as follows: 4X per day, 51 sec per application and maintained in culture in the presence and absence of the ROCK-1 inhibitor, Y26732. Upon completion of the experiment, the cell-seeded scaffolds were stained for actin, tubulin and vimentin and were visualized by confocal microscopy. A) actin distribution in control, non-stimulated cells; B) actin cytoskeleton for control cells in the presence of Y26732 inhibitor; C) actin distribution for US-stimulated cells in the absence of Y26732inhibitor; D) distribution of actin in cells subjected to US stimulation in the presence of Y26732inhibitor; E) tubulin in control cells; F) tubulin distribution in control cells in the presence of Y26732 inhibitor; G) tubulin distribution in US-stimulated cells in the absence of Y26732 inhibitor; H) tubulin in US-stimulated cells with Y26732 inhibitor; I) vimentin distribution in control cells in the absence of Y26732 inhibitor; J) vimentin distribution in control cells in the presence of Y26732 inhibitor; K) vimentin distribution in US-stimulated cells in the absence of Y26732; L) vimentin distribution in US-stimulated cells in the presence of Y26732 inhibitor.

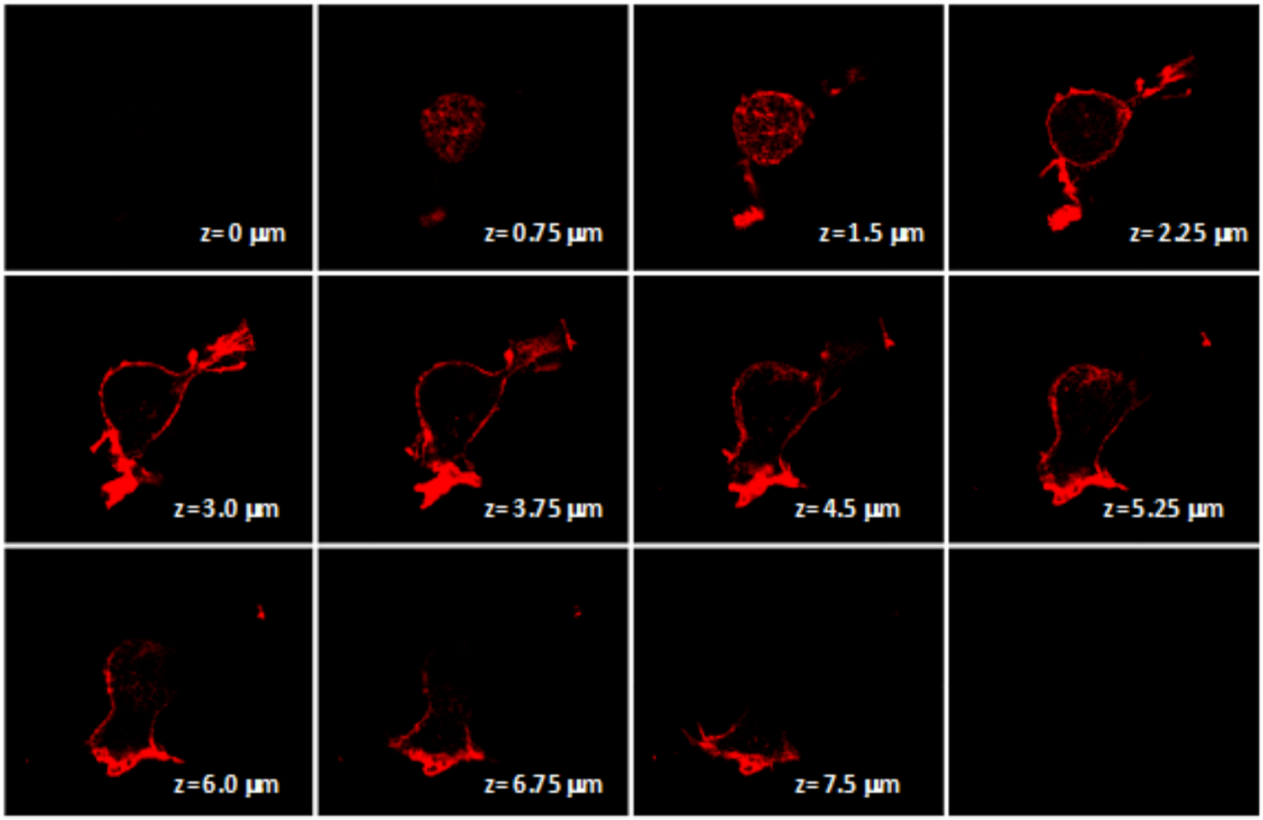

Figure 5A. Visualization of actin cytoskeleton Z stacks montage of non-ultrasound stimulated cells

Montage made out of z slices of images taken from control cells grown on FDL chitosan scaffolds for 3 days in the absence of the actin inhibitor, Y26732.

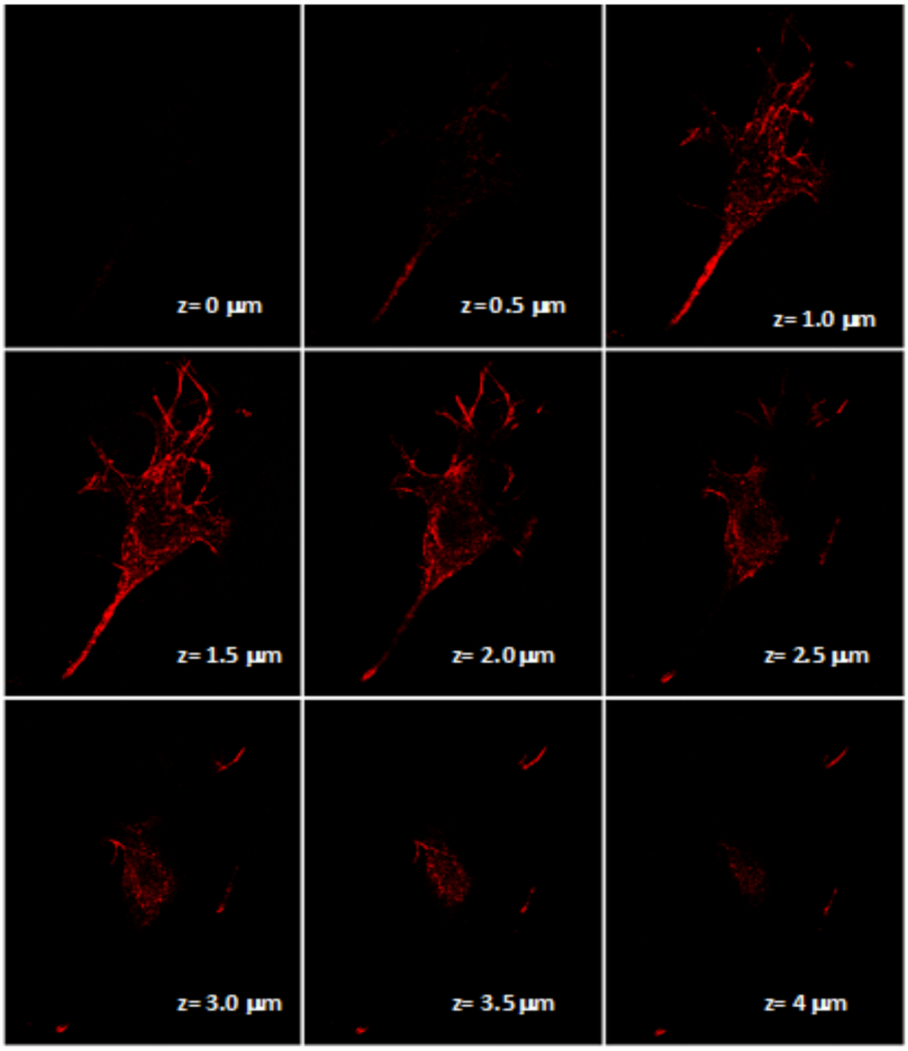

Figure 5B. Visualization of actin cytoskeleton Z stacks montage of non-ultrasound with Y27632 inhibitor

Montage made out of z slices of images taken from control cells grown on FDL chitosan scaffolds for 3 days in the presence of the actin inhibitor, Y26732.

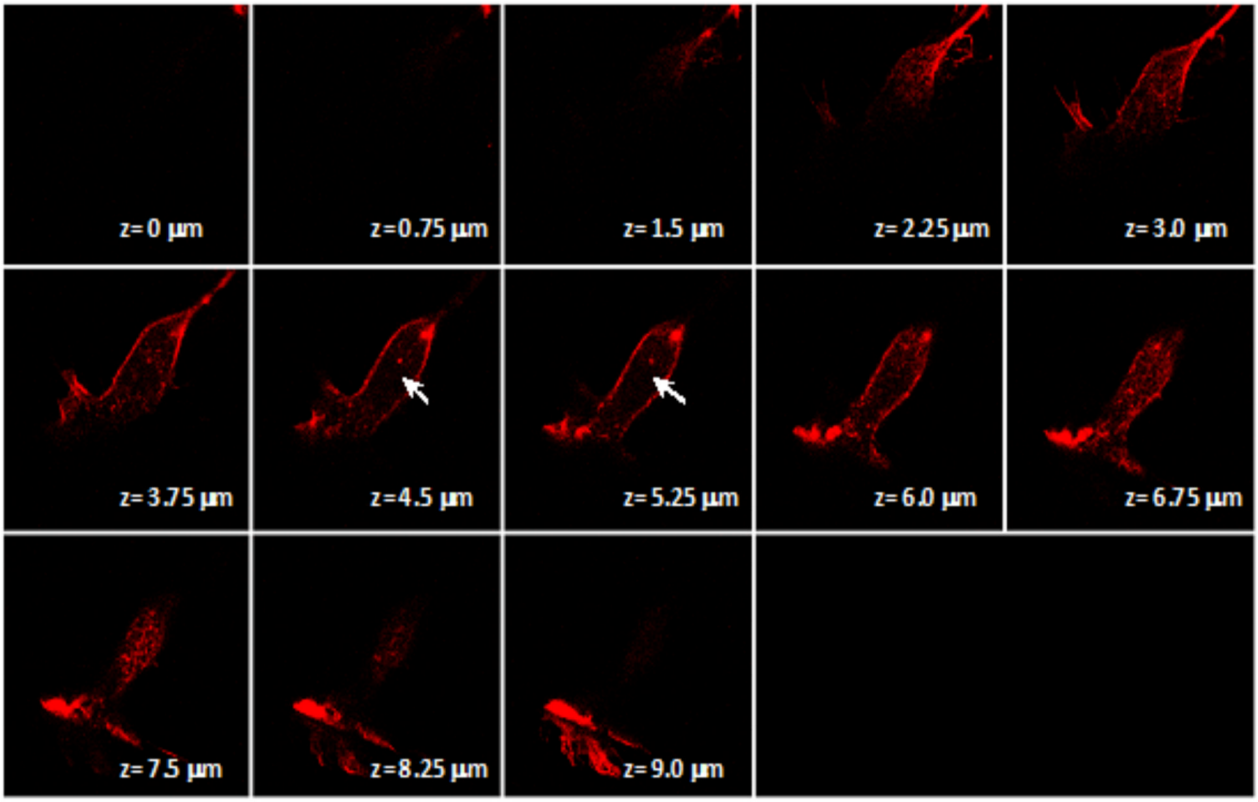

Figure 5C. Visualization of actin cytoskeleton Z stacks montage of ultrasound stimulated cells
Montage made out of the z slices from the confocal images taken from ultrasound stimulated cells without the Y26732 inhibitor.

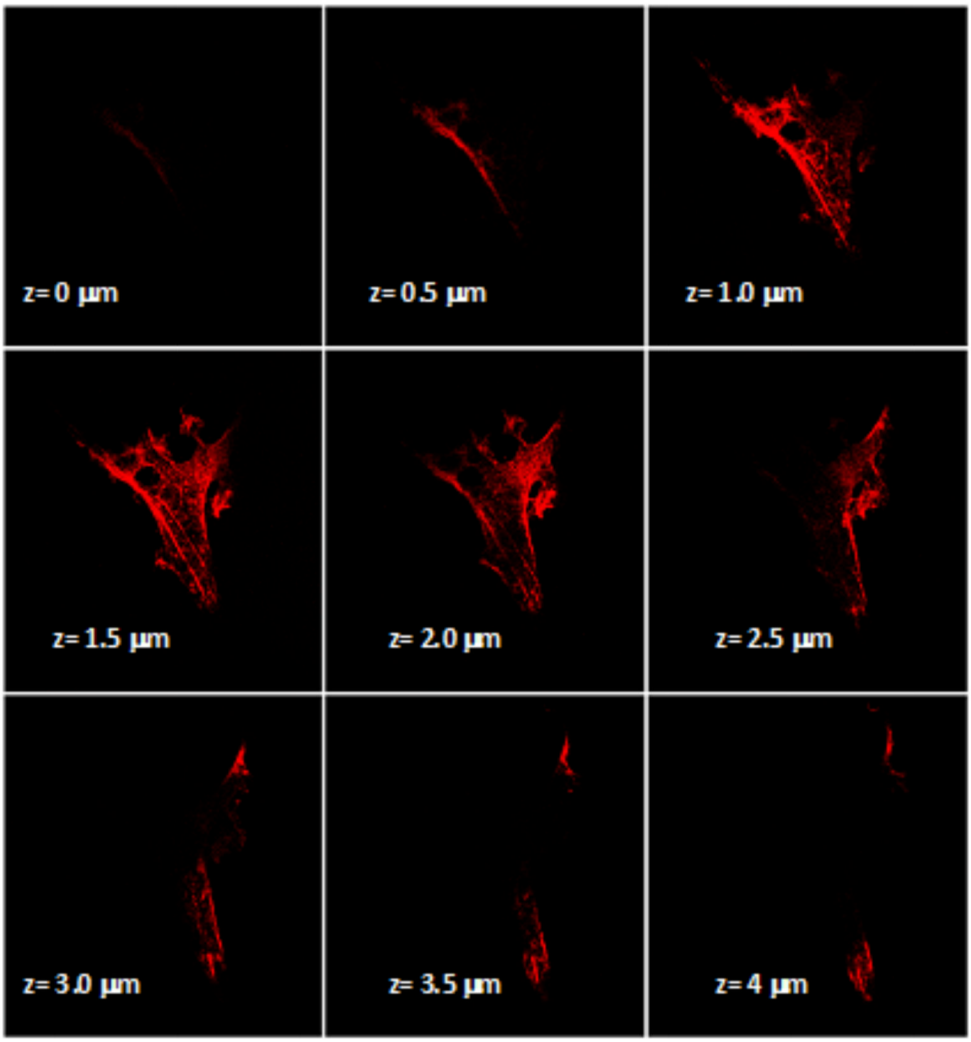

Figure 5D. Visualization of actin cytoskeleton Z stacks montage of ultrasound stimulated cells with Y27632 inhibitor

Montage made out of the z slices from the confocal images of cells taken from ultrasound stimulated cells with the Y26732 inhibitor added.

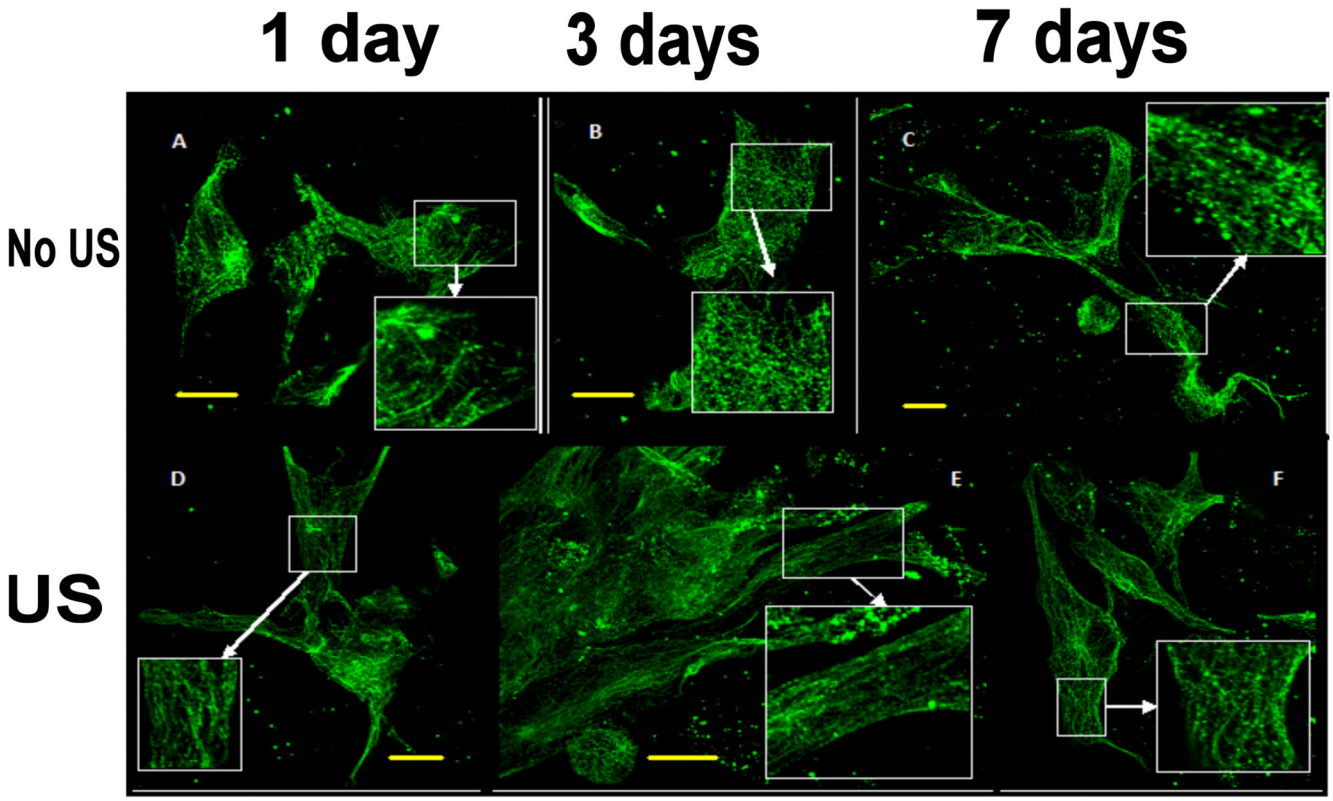

Figure 6. Visualization of the tubulin cytoskeleton organization

US signal was applied to cell-seeded chitosan scaffolds as follows: 4X per day, 51 sec per application and maintained in culture for 1-, 3- and 7-days. Panels A, B and C show the images of control cells after 1, 3 and 7 days, respectively. Panels D, E and F show the image of ultrasound stimulated cells after 1, 3 and 7 days.

Table 1

Sequence of the primers used in RT-PCR

Genes	Accession number	Primers (forward)	Primers (reverse)	Size, bp
mDial	XM_595101	5-TTGCAAGAAAATGTGCAAGC-3	5-AACGATGCTCAGCAGGAACT-3	331
Rho-A	NM_176645	5-AACAGGATTGGTGCTTTTGG-3	5 AGTGCAGAGGAGGGCTGTTA-3	368
ROCK-1	AY_052529	5-GCTCGAGAGAAGGCTGAAAATAG-3	5-CATCTGCCCTTCATTCCCTCTG-3	342
GAPDH	XR_027343	5-ACCCAGAAGACTGTGGATGG-3	5-CCCAGCATCGAAGGTAGAAG-3	323